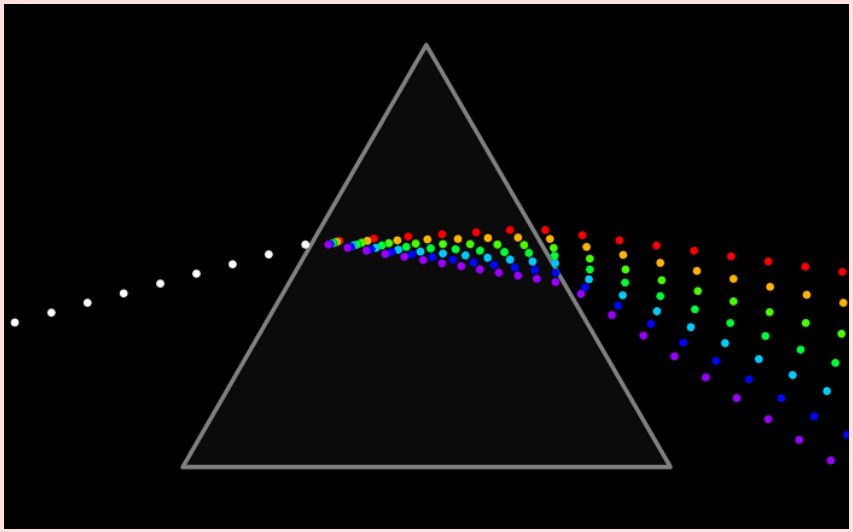
Precision Physics for Fundamental Physics

V.I. Korobov

Joint Institute for Nuclear Research
141980, Dubna, Russia



Dubna, October, 2026

Introduction

What is precision physics?

1. What can we measure with very high precision — frequency!

   Second is currently defined as the duration of 9 192 631 770 periods of the radiation corresponding to the transition between *the two hyperfine levels of the ground state of the caesium 133 atom*.
2. Hydrogen atom, muonic hydrogen, and positronium
3. Precision Spectroscopy of the Hydrogen molecular ions
4. Physics of exotic atoms

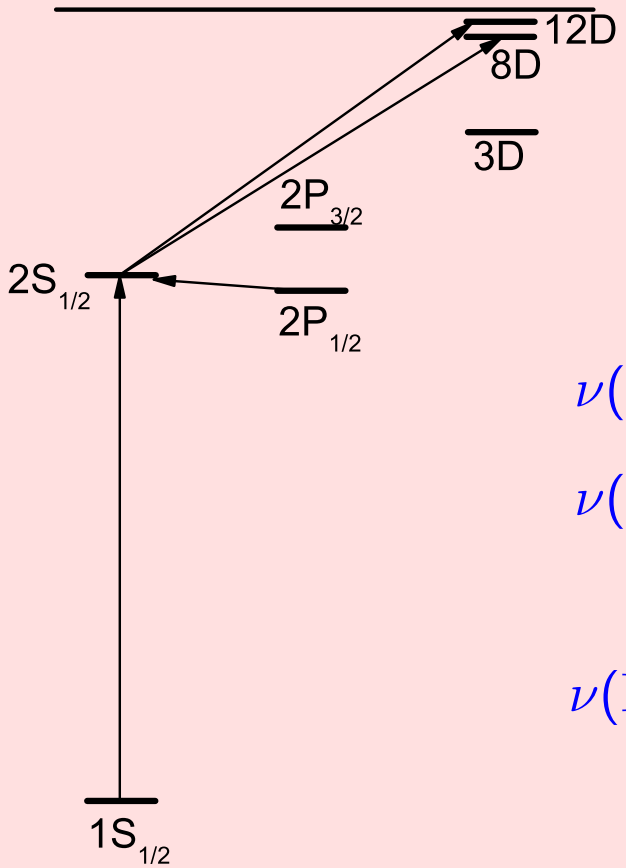
Introduction

What can we get studying precision physics?

1. Tight constrains on new forces
2. Fundamental physical constants
3. Variation of fundamental constants with time.
4. Tests of the CPT invariance
5. Properies of exotic particles like muon, pion, kaon, etc.

Precision physics: Experiment

Rydberg constant from hydrogen atom



$$\nu(2S_{1/2}\text{–}12D_{5/2}) = \ 799\,191\,727.403\,7(47)\ \text{MHz}$$

$$\nu(1S_{1/2}-2S_{1/2}) = 2\,466\,061\,413.187\,018(11)\ \text{MHz}$$

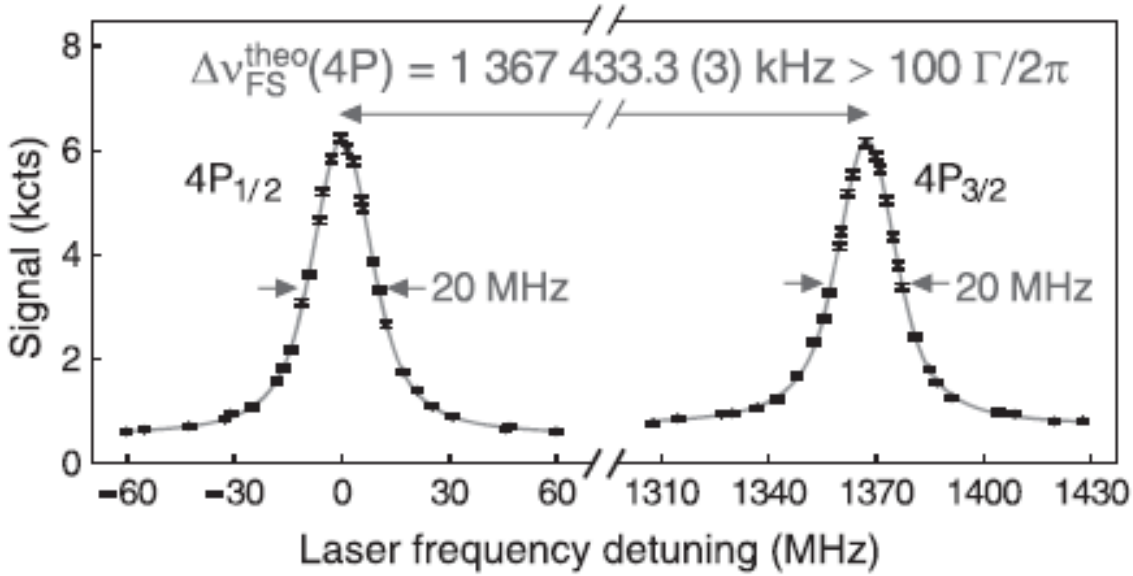
$$\nu(\text{HFS}) = 1\,420.405\,751\,768(2)\ \text{MHz}$$

$$R_\infty c = 3.289\,841\,960\,2500(36) \times 10^{15}\ \text{Hz}$$

Rydberg constant. MPQ experiment, Garching.

$1S$-$4P$ transition.

A. Bayer, *et al.* Science **358**, 79 (2017).

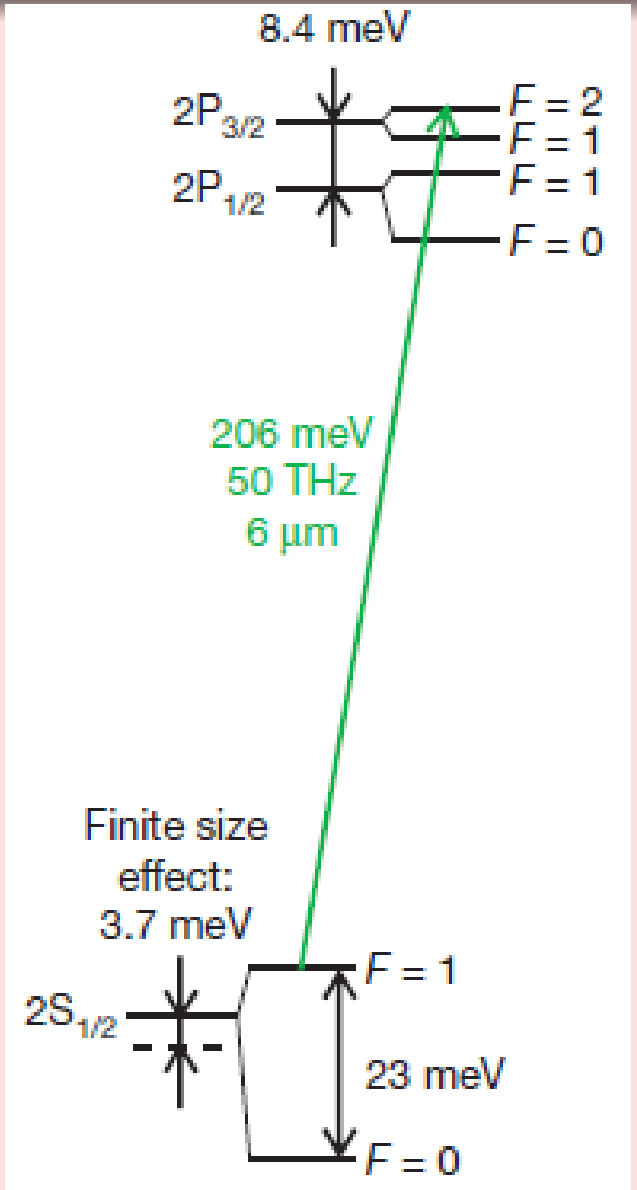


conservation. (**B**) Typical experimental fluorescence signal from a single line scan over the 2S-$4P_{1/2}$ (left) and 2S-$4P_{3/2}$ (right) resonance (black diamonds). The observed line width (full width at half maximum) of ~$2\pi \times 20$ MHz is larger than the natural line width $\Gamma = 2\pi \times 12.9$ MHz because of Doppler and power broadening. The accuracy of our measurement corresponds to almost 1 part in 10,000 of the observed line width. The constant background counts are caused by the decay of 2S atoms inside the detector (*17*). kcts, kilocounts.

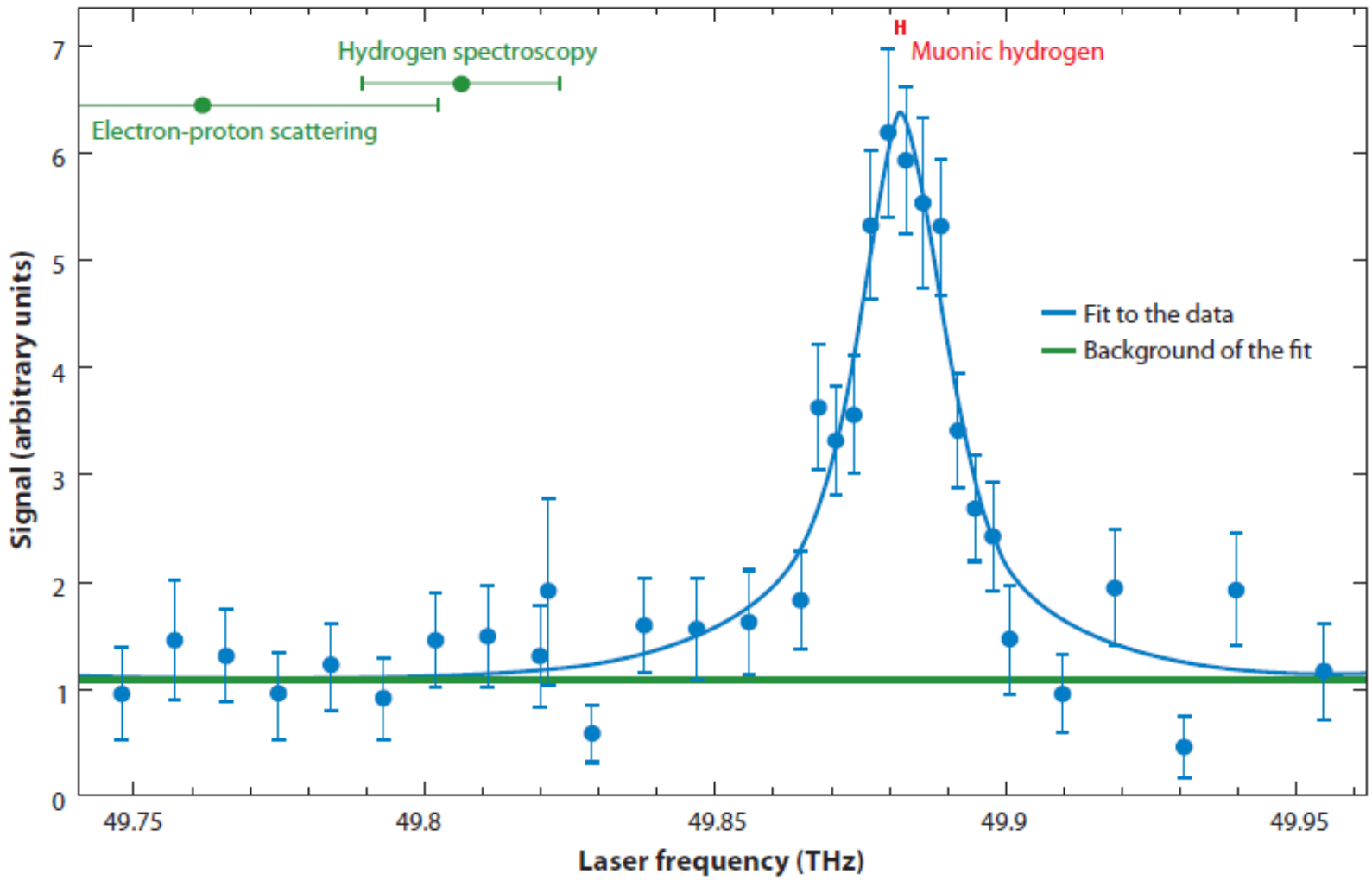
Proton charge radius puzzle. First experiment.

Randolf Pohl, *et al.* (CREMA Collab.)
The Size of the proton.
Nature **466**, 213 (2010).

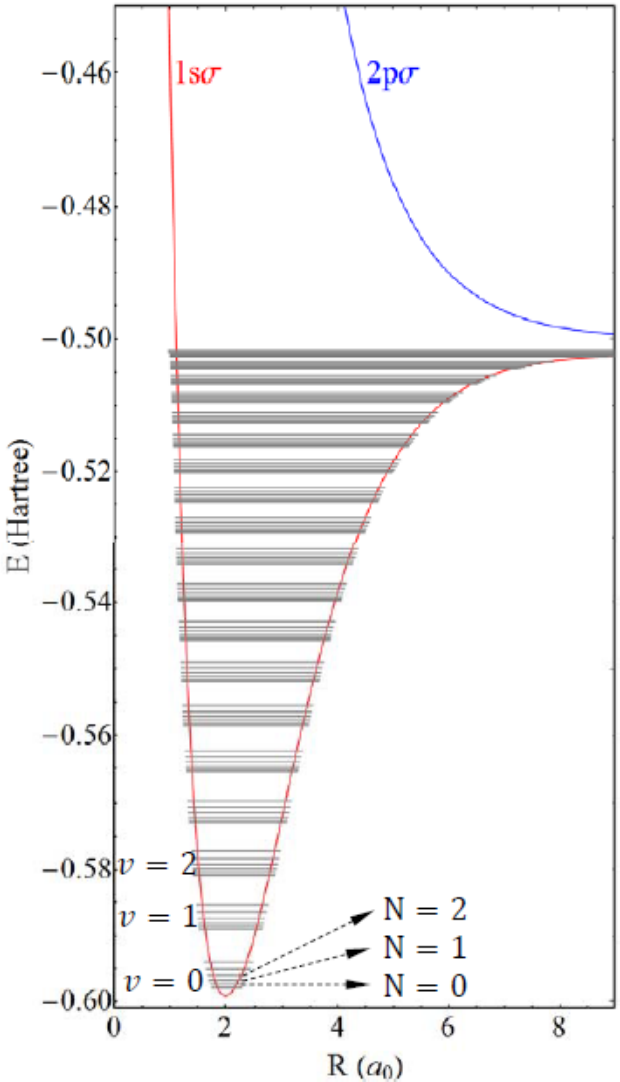
The charge radius of the proton from muonic hydrogen spectroscopy should be $r_p = 0.84184(67)$ fm while the CO-DATA06 recommended value is 5σ off $r_p = 0.8768(69)$ fm



Proton charge radius puzzle



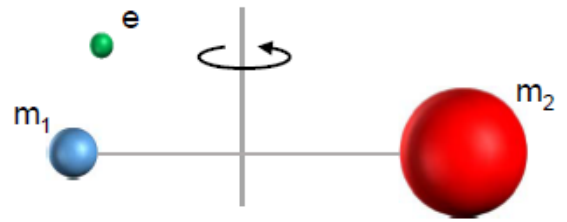
Molecular ion spectroscopy





$$f_{\mathrm{vib}} \propto cR_\infty \, G_{vN,v'N'}(m_e/m_1 + m_e/m_2, \alpha)$$

+ relativity + QED + nuclear charge radii



$$f_{\mathrm{rot}} \propto cR_\infty \, H_{vN,v'N'}(m_e/m_1 + m_e/m_2, \alpha)$$

+ relativity + QED + nuclear charge radii

Molecular ion spectroscopy in the RF trap

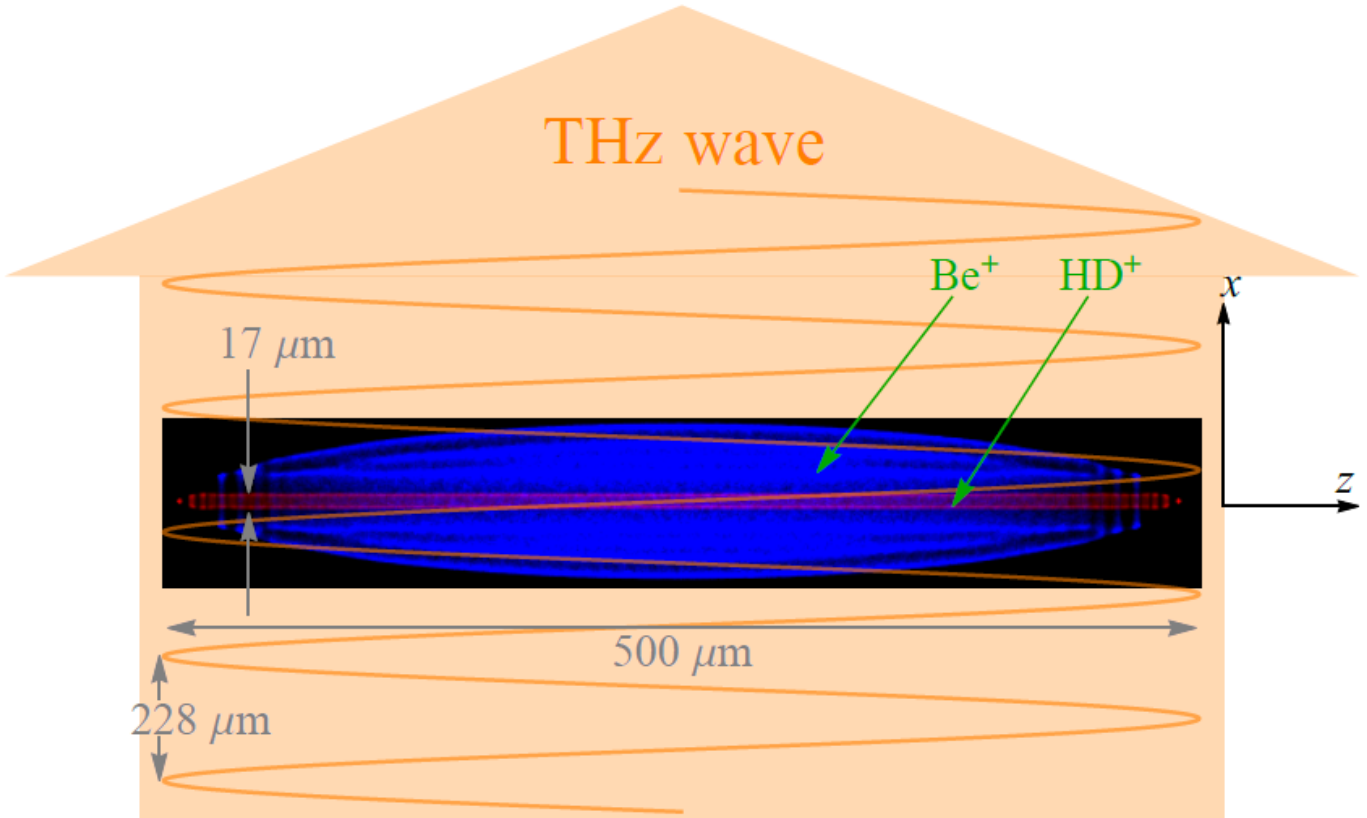
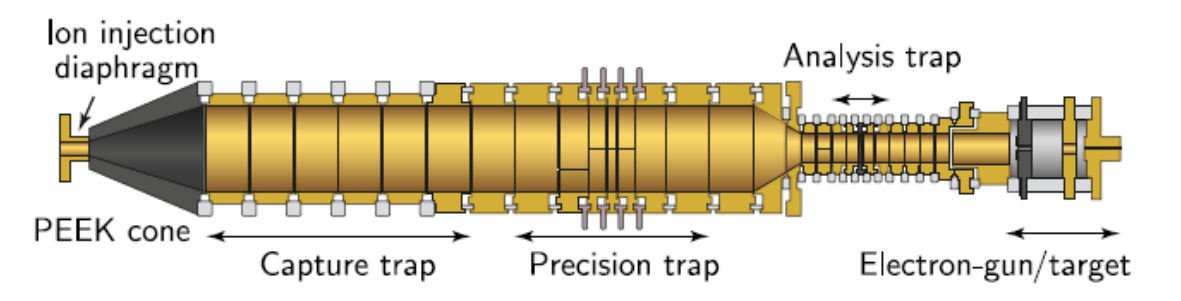


FIG. 1. **Principle of the Lamb-Dicke rotational spectroscopy of sympathetically cooled molecular ions.** The ion cluster is prolate, and the sympathetically cooled ions exhibit a relatively small motional range in the directions x, y perpendicular to the trap axis z. The spectroscopy radiation propagates perpendicular to z. The ion cluster image is a time average of ion trajectories

Penning trap experiments

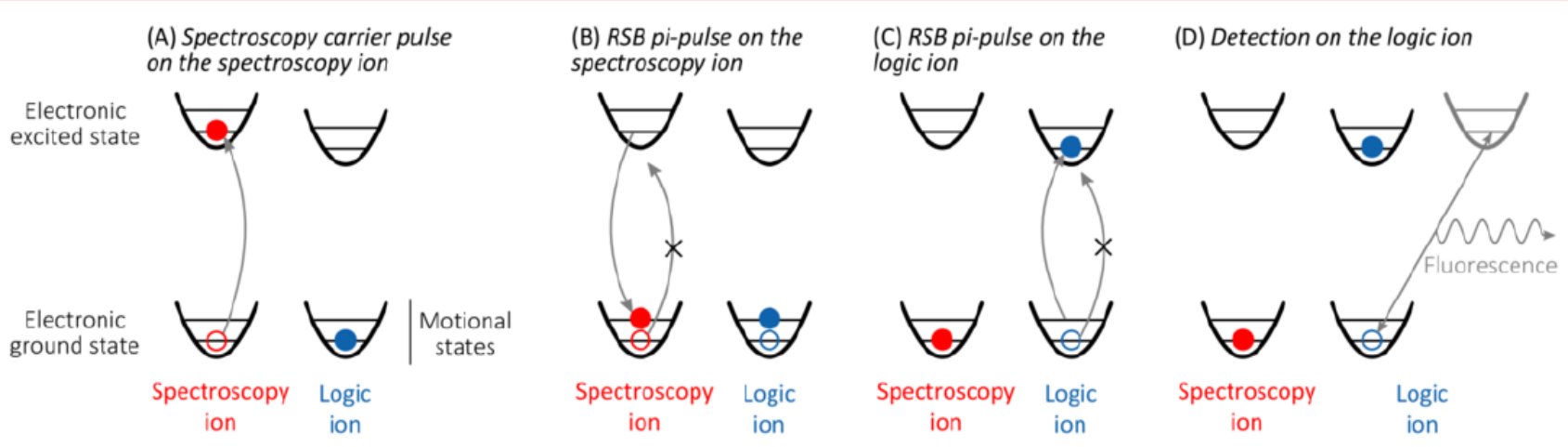


The ALPHATRAP tower. The precision trap is used for high-precision spectroscopy and the analysis trap is used for the state determination.

Precision measurements:

- electron g-factor measurements;
- proton and other nuclei magnetic moments;
- Mass ratios;
- Vibrational and HFS transitions in the molecular ions.

Quantum Logic Spectroscopy



Scheme of quantum logic spectroscopy: The filled circles denote the ion's motional and electronic state in case of the successful spectroscopy pulse in (A), the empty circles represent the state in case the spectroscopy pulse in (A) did not excite the spectroscopy ion.

- Atomic ion clocks: $Al^+(S)$–$Be^+(L)$
- Molecular ion spectroscopy
- State preparation

Precision physics: Theory

Three-body problem: Helium atom

PHYSICAL REVIEW A **98**, 012510 (2018)

Nonrelativistic energy levels of helium atoms

D. T. Aznabaev,[1,2,3] A. K. Bekbaev,[1,4] and Vladimir I. Korobov[1,5]

TABLE II. Nonrelativistic energies of the S, P, D, and F states of a helium atom. N is the number of basis functions. The two lines represent two consecutive calculations with the largest basis sets to show convergent digits. The third line presents calculations by Drake and Yan [23].

State	N	E_{nr}	State	N	E_{nr}
1^1S	18000	−2.90372 43770 34119 59831 11592 45194 40432	4^1S	14000	−2.03358 67170 30725 44743 92926 44363 64
1^1S	22000	−2.90372 43770 34119 59831 11592 45194 40443	4^1S	18000	−2.03358 67170 30725 44743 92926 44363 87
2^1S	18000	−2.14597 40460 54417 41580 50289 75461 918	4^3S	14000	−2.03651 20830 98236 29958 03780 71617 853
2^1S	22000	−2.14597 40460 54417 41580 50289 75461 921	4^3S	16000	−2.03651 20830 98236 29958 03780 71617 874
	[23]	−2.14597 40460 5443(5)			
2^3S	14000	−2.17522 93782 36791 30573 89782 78206 81124	4^1P	18000	−2.03106 96504 50240 71475 89314 36090 3
2^3S	16000	−2.17522 93782 36791 30573 89782 78206 81125	4^1P	22000	−2.03106 96504 50240 71475 89314 36094 1
	[23]	−2.17522 93782 367912(1)		[23]	−2.03106 96504 5024(3)
2^1P	18000	−2.12384 30864 98101 35924 73331 42354	4^3P	18000	−2.03232 43542 96630 33195 38824 67087
2^1P	22000	−2.12384 30864 98101 35924 73331 42374	4^3P	22000	−2.03232 43542 96630 33195 38824 67103
	[23]	−2.12384 30864 98092(8)		[23]	−2.03232 43542 9662(2)
2^3P	16000	−2.13316 41907 79283 20514 69927 63793	4^1D	22000	−2.03127 98461 78684 99621 39438 073
2^3P	18000	−2.13316 41907 79283 20514 69927 63806	4^1D	26000	−2.03127 98461 78684 99621 39438 143
	[23]	−2.13316 41907 7927(1)		[23]	−2.03127 98461 78687(7)
3^1S	18000	−2.06127 19897 40908 65074 03499 37089 2816	4^3D	18000	−2.03128 88475 01795 53802 34920 591
3^1S	22000	−2.06127 19897 40908 65074 03499 37089 2824	4^3D	22000	−2.03128 88475 01795 53802 34920 630
				[23]	−2.03128 88475 01795(3)
3^3S	14000	−2.06868 90674 72457 19199 65329 11291 75048	4^1F	18000	−2.03125 51443 81748 60863 20824 071
3^3S	16000	−2.06868 90674 72457 19199 65329 11291 75049	4^1F	22000	−2.03125 51443 81748 60863 20824 079
				[23]	−2.03125 51443 81749(1)

Nonrelativictic QED (NRQED)

Concept of NRQED

QED

$$\mathcal{L}_{\rm QED} = \bar{\psi}\left[(i\partial - e\,A)\,\gamma - m\right]\psi - \frac{1}{4}F_{\mu\nu}F^{\mu\nu},$$

$$\Downarrow$$

Nonrelativistic QED

$$\mathcal{L}_{\rm NRQED}$$

$$\Downarrow$$

Effective Hamiltonian

$$H_{\rm eff} = \sum_i \frac{\mathbf{P}_i^2}{2m_i} + e^2 \sum_{j>i} \frac{Z_i Z_j}{r_{ij}} + \text{higher order corrections}$$

(Here $\mathbf{P}_i = \mathbf{p}_i + e\mathbf{A}$)

Nonrelativistic QED Lagrangian

The Lagrangian for NRQED is built out nonrelativistic (two-component) Pauli spinor fields ψ for each of the electron, positron, muon, proton, etc. Photons are treated in the same fashion as in QED.

$$
\begin{aligned}
L_{\rm eff} = &-\tfrac{1}{2}(E^2 - B^2) + \psi_e^* \left(i\partial_t - e\varphi + \frac{\mathbf{D}^2}{2m} + \frac{\mathbf{D}^4}{8m^3} + \ldots \right) \psi_e \\
&+ \psi_e^* \left(c_F \frac{e}{2m} \boldsymbol{\sigma}\mathbf{B} + c_D \frac{e}{8m^2} \big[\mathbf{DE}\big] + c_S \frac{e}{8m^2} \big\{ \boldsymbol{\sigma} \cdot [i\mathbf{D} \times \mathbf{E}] \big\} \right) \psi_e \\
&+ \text{higher order terms} + \text{muon, proton, etc.} \\
&- \frac{d_1}{m_e m_\ell} (\psi_e^* \boldsymbol{\sigma}_e \psi_e)(\psi_\ell^* \boldsymbol{\sigma}_\ell \psi_\ell) + \frac{d_2}{m_e m_\ell} (\psi_e^* \psi_e)(\psi_\ell^* \psi_\ell) + \ldots
\end{aligned}
$$

where $\mathbf{D} = \boldsymbol{\nabla} - ie\mathbf{A}$.

Wilson coefficients

Wilson coefficients for the electron interactions with external field:

$$c_D = 1 + 2a_e + \frac{\alpha}{\pi}\frac{8}{3}\left[\ln\left(\frac{m}{2\Lambda}\right) + \frac{5}{6} - \frac{3}{8}\right],$$

$$c_S = 1 + 2a_e,$$

$$c_F = 1 + a_e.$$

Wilson coefficients for contact interactions:

$$d_1 = (Z\alpha)^2 \frac{2}{m_e^2 - m_\ell^2} \ln\left(\frac{m_e}{m_\ell}\right),$$

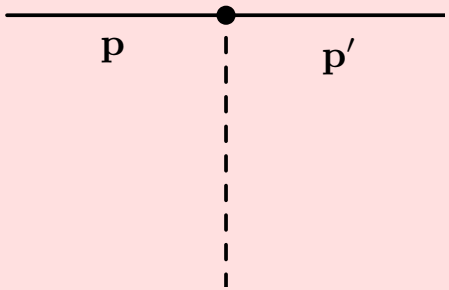
$$d_2 = (Z\alpha)^2 \left\{\frac{7}{3} - 2\ln\left(\frac{m}{2\Lambda}\right) + \frac{2}{m_e^2 - m_\ell^2}\left[m_e^2 \ln\left(\frac{m_\ell}{\mu}\right) - m_\ell^2 \ln\left(\frac{m_e}{\mu}\right)\right]\right\}.$$

Here μ is the reduced mass of a pair.

Examples of basic interactions in NRQED. Vertices.

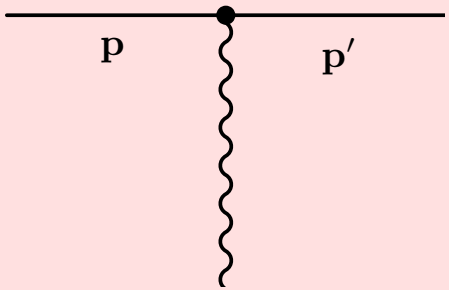
Coulomb

e



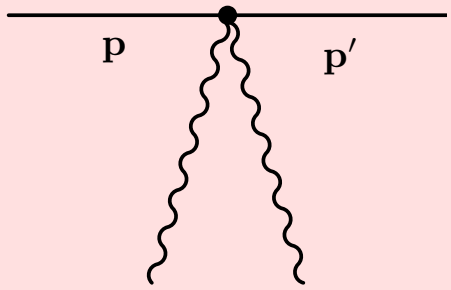
"dipole"

$-e\left[\frac{\mathbf{p}'+\mathbf{p}}{2m}\right]$



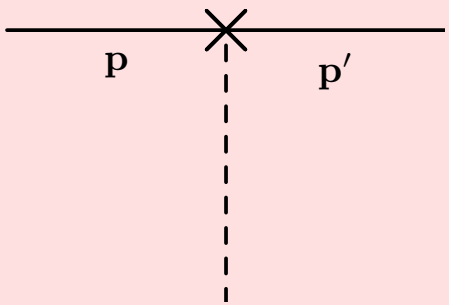
$\mathbf{A}^2$

$e^2\left[\frac{\delta^{ij}}{2m}\right]$



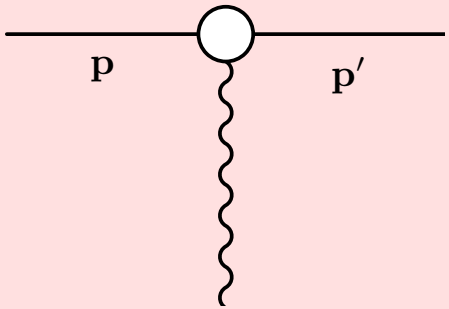
Darwin's

$-e\left[\frac{1}{8m^2}\right]\mathbf{q}^2$



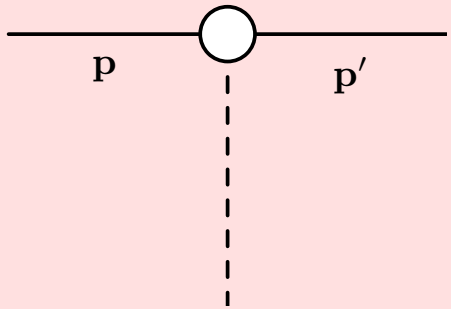
Fermi's

$e\left[\frac{i}{2m}\right](\mathbf{q}\times\boldsymbol{\sigma})$



spin–orbit

$e\left[\frac{i}{4m^2}\right](\mathbf{p}'\times\mathbf{p})\cdot\boldsymbol{\sigma}$



Here $\mathbf{q}=\mathbf{p}'-\mathbf{p}$ is a transferred impulse of the particle.

NRQED propagators

A natural choice of a gauge for the electromagnetic field is the Coulomb gauge ($\mathbf{kA} = 0$)

$$\begin{cases} G^{00} = \dfrac{1}{\mathbf{k}^2}\,, & \text{— the Coulomb photon propagator,} \\ G^{ij} = \dfrac{\delta_{ij} - k_i k_j/\mathbf{k}^2}{k^2 + i\varepsilon}\,, & \text{— the transverse photon propagator,} \\ G^{0i} = G^{i0} = 0, \qquad i,j = 1,2,3. \end{cases}$$

For exchange photons $k_0 \approx m\alpha^2$ and

$$G^{ij} \approx -\frac{1}{\mathbf{k}^2}\left[\delta_{ij} - \frac{k_i k_j}{\mathbf{k}^2}\right].$$

Propagators for massive particles

$$\frac{1}{E - \mathbf{p}^2/(2m) + i\varepsilon}\,.$$

Zero-order approximation

Zero-order Lagrangian is

$$L_{\rm eff}^{(0)} = -\frac{1}{2}(E^2 - B^2) + \sum_n \psi_n^* \left(i\partial_t - eZ_n\varphi + \frac{\mathbf{D}^2}{2m_n} \right) \psi_n \,.$$

By variation of field functions ψ_n and quantization of the electromagnetic field, one gets the nonrelativistic Hamiltonian of a system of particles interacting with an electromagnetic field:

$$\check{H}_0 = \sum_i \frac{\mathbf{P}_i^2}{2m_i} + e^2 \sum_{j>i} \frac{Z_i Z_j}{r_{ij}} + \sum_{\lambda=1,2} \int d^3k\, k\, a_{k\lambda}^+ a_{k\lambda}. \qquad (*)$$

Here $\mathbf{P}_i = \mathbf{p}_i + eZ_i\mathbf{A}$. Operators $\mathbf{A}(\mathbf{r})$ are presented in terms of photon creation and annihilation operators

$$\mathbf{A}(\mathbf{r}) = (2\pi)^{-3/2} \int \frac{d^3k}{\sqrt{2k}} \left(a_{k\lambda}^+ e^{-i\mathbf{kr}} + a_{k\lambda} e^{i\mathbf{kr}} \right) \mathbf{e}_\lambda.$$

Hamiltonian (*) is a convenient starting point for building up the nonrelativistic quantum electrodynamics (NRQED) in the Hamiltonian form.

Nonstationary perturbation theory

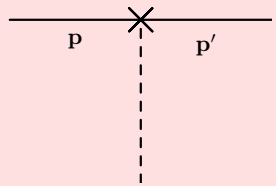
Let $H = H_0 + V$, then we can expand K in increasing powers of V:

$$K(2,1) = K_0(2,1) + K^{(1)}(2,1) + K^{(2)}(2,1) + \dots$$

where $K_0(2,1)$ is a propagator (or a Green's function) of the unperturbed Hamiltonian:

$$K_0(2,1) = e^{-iH_0(t_2-t_1)},$$
$$[i\partial/\partial t_2 - H_0(2)]\, K_0(2,1) = i\delta(2,1).$$

For instantaneous interaction:

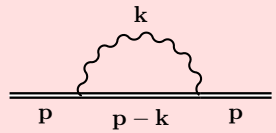


$$K^{(1)}(2,1) = -i \int K_0(2,3) V(3) K_0(3,1)\, d\tau_3,$$

For a transverse photon:

$$K^{(1)}(2,1) = -i \int K_0(2,4) V(4) G(4,3) K_0(4,3) V(3) K_0(3,1) d\tau_3 d\tau_4,$$

Functions $V(3)$ and $V(4)$ are some vertex functions of interaction with the electro-magnetic field.



Hydrogen molecular ion H_2^+

Hydrogen molecular ion H_2^+

[V.I. Korobov, J.-Ph. Karr, PRA **104**, 032806 (2021)]

Contributions to the *ab initio* spin-averaged transition frequency:
$(v = 1, N = 0) \to (v' = 3, N' = 2)$

Relative order	Contribution (kHz)	Origin
α^0	124 485 554 550.93	Nonrelativistic 3-body Schrödinger equation
α^2	2 002 698.73	Relativistic corrections in Breit–Pauli approximation; finite nuclear radii
α^3	−521 345.53	Leading-order one-loop radiative corrections
α^4	−3 689.05	One- and two-loop radiative corrections relativistic corrections
α^5	228.65	Up to three-loop radiative and WK corrections
α^6	−1.62	One- and two-loop radiative diagrams; WK
other	0.54	Muon and hadron vacuum polarization
total	124 487 032 442.46	Total transition energy

Relative theoretical uncertainty: $u_r \approx 7.5 \times 10^{-12}$

Transition intensities

HD^+ ions

The dominant transitions are the dipole E1 transitions between ro-vibrational states. Selection rule: $L \to L \pm 1$. Spontaneous emission rate is about $6\ s^{-1}$ and the natural line width is about 1 Hz.

H_2^+ ions

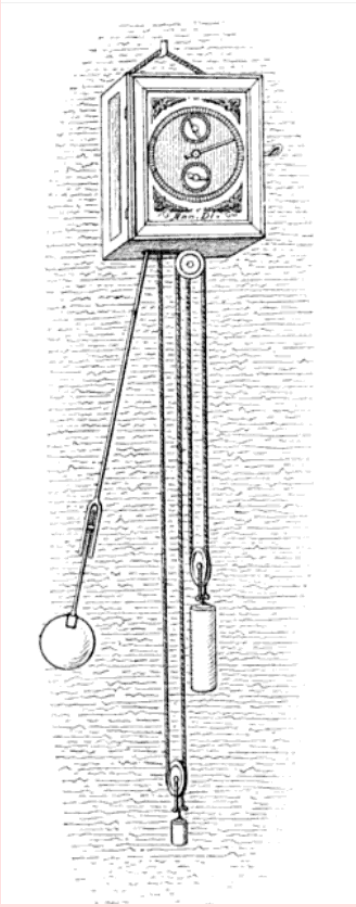
The dominant transitions are the quadrupole E2 ro-vibrational transitions. Selection rule: $L \to L-2, L, L+2$. Spontaneous emission rate is about $10^{-7}\ s^{-1}$ and the natural line width is about 10^{-8} Hz.

There are also the E1 forbidden dipole transitions, which connects "ortho" and "para" states of H_2^+. These transitions are three orders of magnitude weaker than the E2 transitions.

Applications for fundamental physics

First standards of length and time

Second



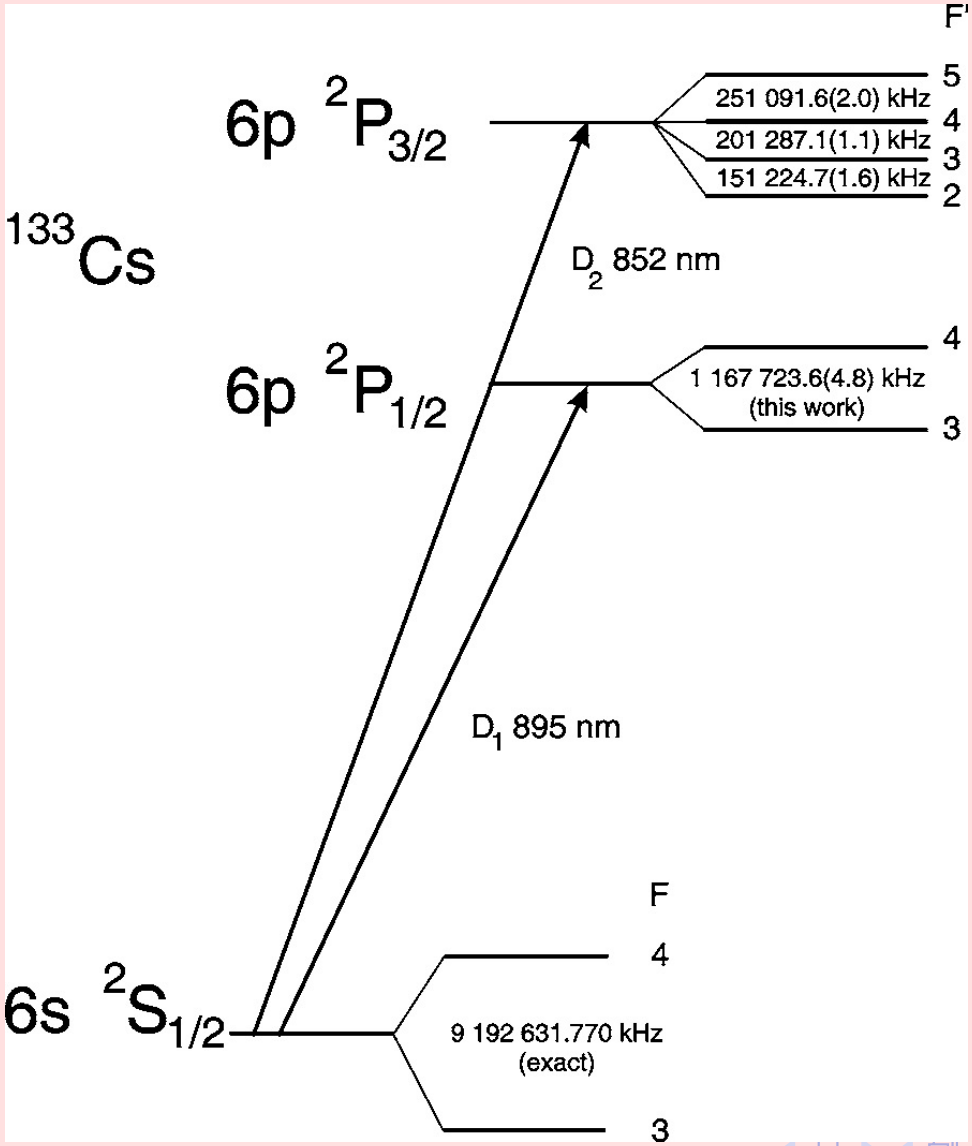
First pendulum clock was invented in 1656 by Christiaan Huygens.

Meter



Platinum-Iridium meter bar.

Spectrum of cesium atom. Atomic clocks.



Main characteristic for frequency standards

- Quality factor (Q): The ratio of the transition frequency to the width of the spectral line.
- Accuracy/ Systematic Uncertainty
  - Zeeman effect
  - BBR shift and differential Stark polarizability
  - gravitational redshift
  - Doppler shift and broadening
- Stability: ability to keep the same frequency over a long period of time

Comparison of various optical clocks

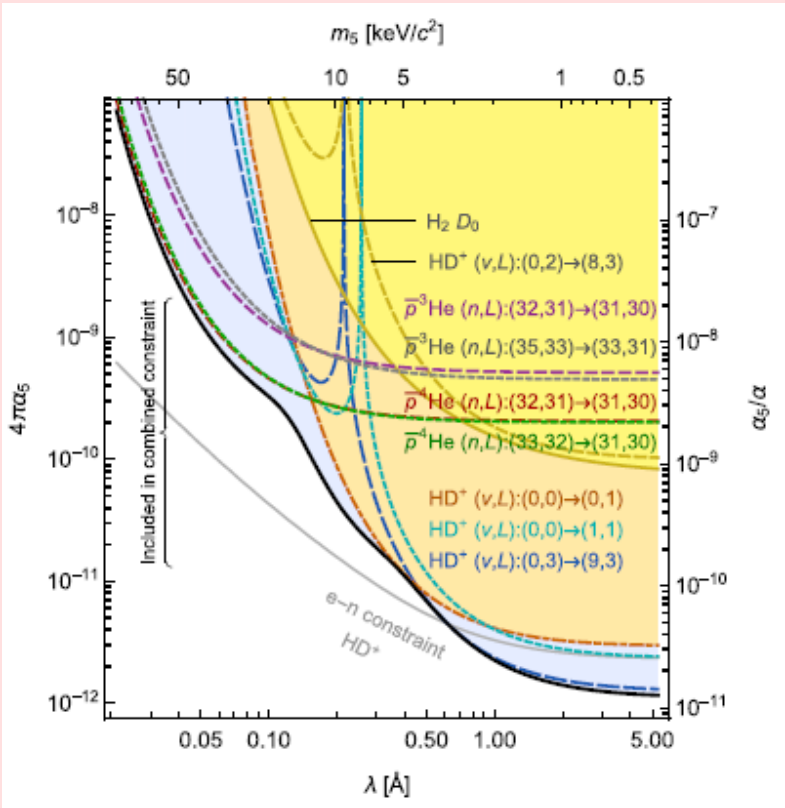
	^{87}Sr	$^{171}Yb^+$	H_2^+
Optical transition	$5s^2(^1S_0 \to {}^3P_0)$	$6s(^2S_{1/2} \to {}^2F_{7/2})$	$(0,2)_F \to (1,2)_F$
Frequency (Hz)	$429 \cdot 10^{12}$	$642 \cdot 10^{12}$	$65 \cdot 10^{12}$
Natural Width (Hz)	10^{-3}	10^{-8}	10^{-8}
Differential polarizability $\Delta\alpha_0$ (in a.u.)	145	16	0.738
Zeeman effect	$\propto B^2$	$\propto B^2$	$\propto B$ $\Delta g_J/g_J \sim 10^{-6}$

New forces beyond SM

Yukawa-type interaction:

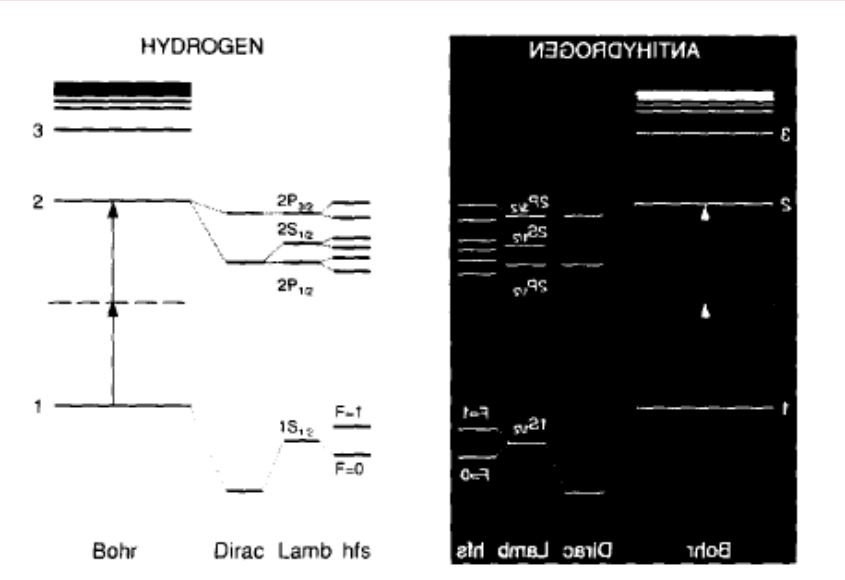
$$V_{\alpha_5,\lambda}(r) = \hbar c \alpha_5 A_1 A_2 \frac{e^{-r/\lambda}}{r},$$

where A_1 and A_2 are nucleon numbers as charges of the hypotetical interaction.



CPT tests

Hydrohen — Antihydrogen



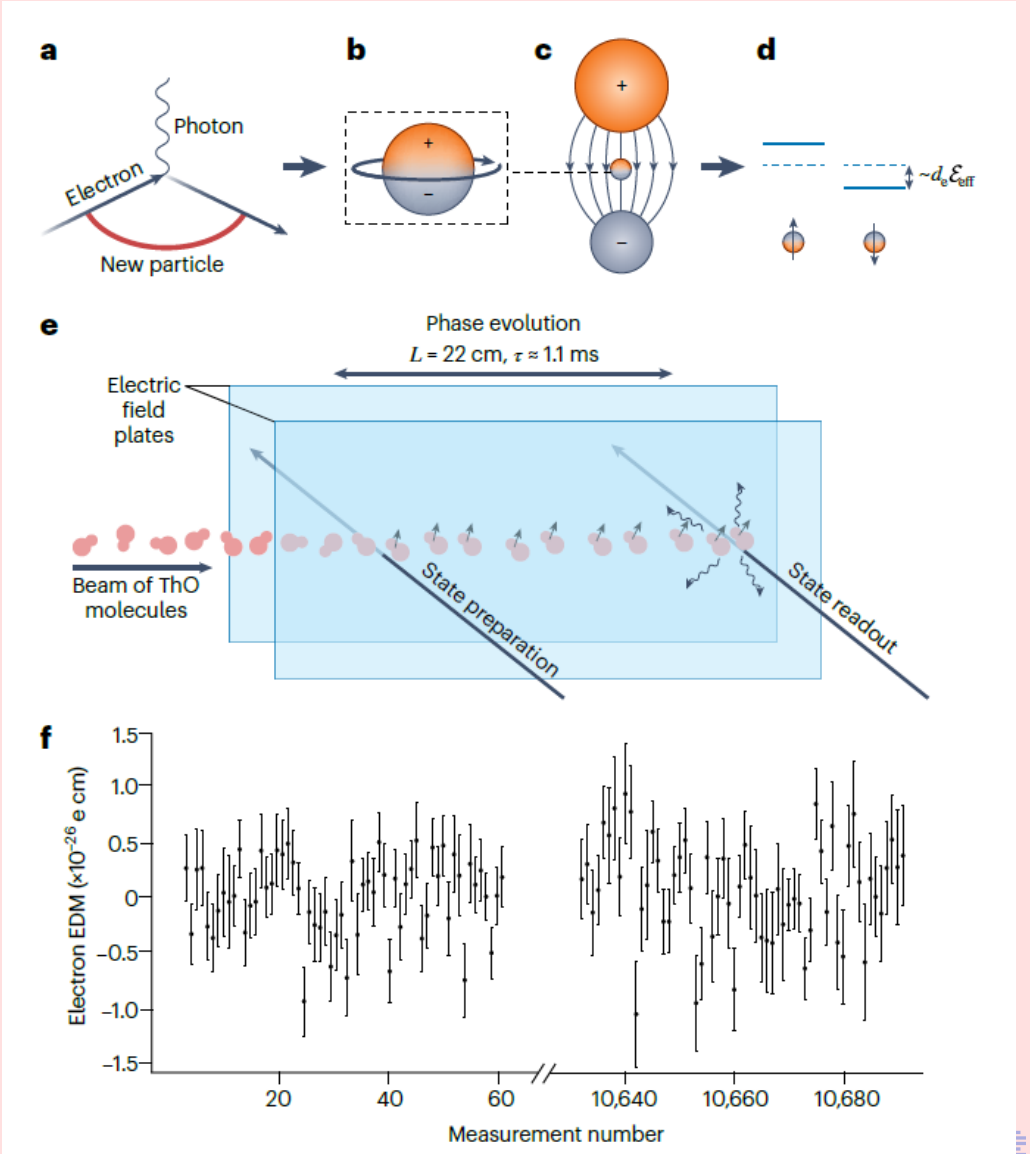
Antihydrogen ion $\bar{p}\bar{p}e^+$ in the Penning trap

- The atom is neutral.
- In case of the ion, no interaction with the trap walls
- The life-time of an ion inside the trap can be up to several months!

CP-violation. EDM. ACME experiment

electron EDM bounds:
$|d_e| < 1.1 \times 10^{-29}$ e cm

mass constrain:
$\Lambda > 30$ TeV



HD^+. Theory and experiment

[V. Korobov, J.-Ph. Karr PRA **104**, 032806 (2021)]
[S. Schiller et al. Nature **581**, 152 (2020)]
[J C J Koelemeij et al. Science **369**, 1238 (2020)]
[S. Schiller et al. Nature Physics **17**, 569 (2021)]

Theoretical and experimental spin-averaged transition frequencies (in kHz). CODATA18 values of fundamental constants were used in the calculations.

$(L,v)\to(L',v')$	theory	experiment
$(0,0)\to(1,0)$	1 314 925 752.932(19)	1 314 925 752.910(17)
$(0,0)\to(1,1)$	58 605 052 163.9(0.5)	58 605 052 164.24(86)
$(3,0)\to(3,9)$	415 264 925 502.8(3.3)	415 264 925 501.8(1.3)

Results

Reduced mass $\mu = \dfrac{m_p m_d}{(m_p + m_d) m_e}$ inferred from the HD^+ ion spectroscopy

	μ
CODATA18	1223.899 228 722(51)
$(0,0) \to (0,1)$	$1223.899\,228\,743(16)_{exp}(17)_{th}$
$(0,0) \to (1,1)$	$1223.899\,228\,707(17)_{exp}(17)_{th}$
$(3,0) \to (3,9)$	$1223.899\,228\,730(04)_{exp}(17)_{th}$
	$1223.899\,228\,730(04)_{exp}(17)_{th}$

Relative uncertainty: $u_r(\mu) = 1.4 \times 10^{-11}$.

Results

Reduced mass $\mu = \dfrac{m_p m_d}{(m_p + m_d) m_e}$ inferred from the HD^+ ion spectroscopy

	μ
CODATA18	1223.899 228 722(51)
$(0,0) \to (0,1)$	$1223.899\,228\,743(16)_{exp}(17)_{th}$
$(0,0) \to (1,1)$	$1223.899\,228\,707(17)_{exp}(17)_{th}$
$(3,0) \to (3,9)$	$1223.899\,228\,730(04)_{exp}(17)_{th}$
	$1223.899\,228\,730(04)_{exp}(17)_{th}$

Relative uncertainty: $u_r(\mu) = 1.4 \times 10^{-11}$.

Mass ratios from spectroscopy and Myers' experiment:

$$m_p/m_e = 1836.152673476(44), \qquad m_d/m_e = 3670.482967763(88),$$

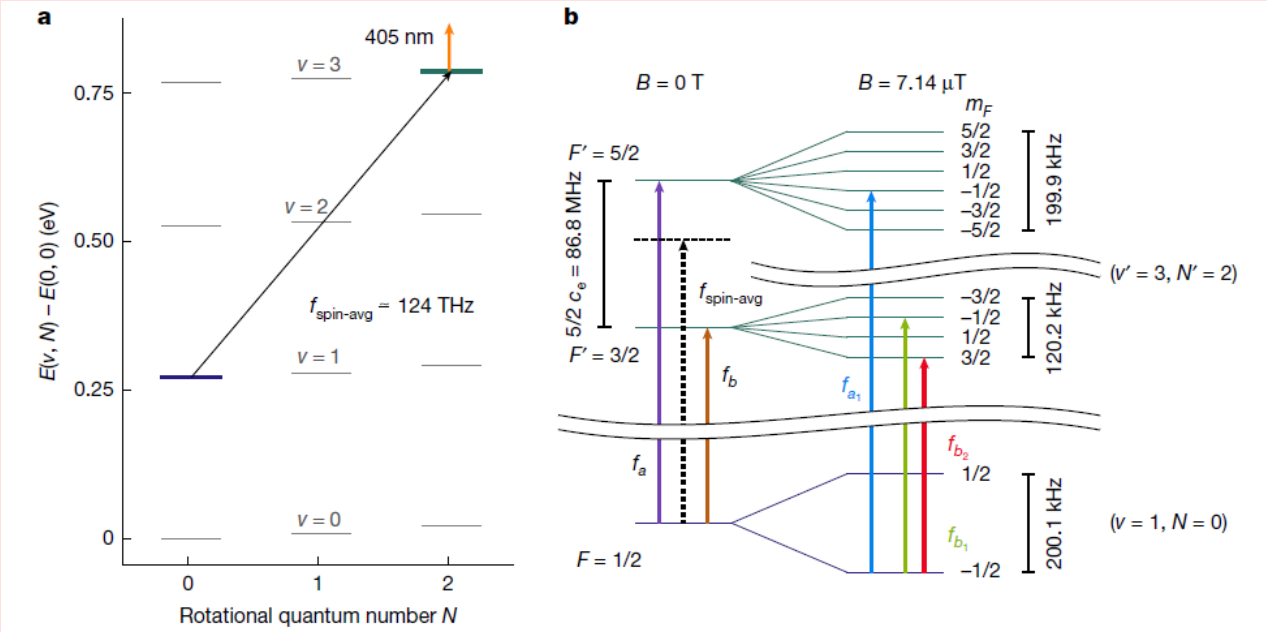
and the new CODATA22 value is $m_p/m_e = 1836.152673426(32)$.

CODATA18 vs CODATA22

quantity	symbol	value	uncertainty
proton rms charge radius	r_p	$0.8414(19)\times10^{-15}$ m	2.2×10^{-3}
		$0.84075(64)\times10^{-15}$ m	7.6×10^{-4}
Rydberg constant	$R_\infty c$	3 289 841 960.2500(64) MHz^{-1}	1.9×10^{-12}
		3 289 841 960.2500(36) MHz^{-1}	1.1×10^{-12}
proton-electron mass ratio	$\mu = m_p/m_e$	1836.152 673 43(11)	6.0×10^{-11}
		1836.152 673 426(32)	1.7×10^{-11}

Quadrupole spectroscopy of H_2^+ in the RF trap

[S. Schiller et al, Nature **644**, 69–75 (2025)]



HFS transition frequencies:

$$f_a^{\rm expt} = 124\,487\,067\,172.9(6)\text{kHz}$$

$$f_b^{\rm expt} = 124\,486\,980\,347.5(8)\text{kHz}$$

$$m_p/m_e = 1\,836.152\,673\,414(47).$$

Physics of exotic atoms

Muon Catalysed Fusion

Reactions:

$$d + t \longrightarrow {}^4He + n + 17{,}6\ МэВ,$$

$$d + d \longrightarrow {}^3He + n + 3{,}3\ МэВ,$$

$$d + d \longrightarrow t + p + 4{,}0\ МэВ,$$

$$p + d \longrightarrow {}^3He + \gamma + 5{,}5\ МэВ.$$

Muon Catalysis Fusion Cycle

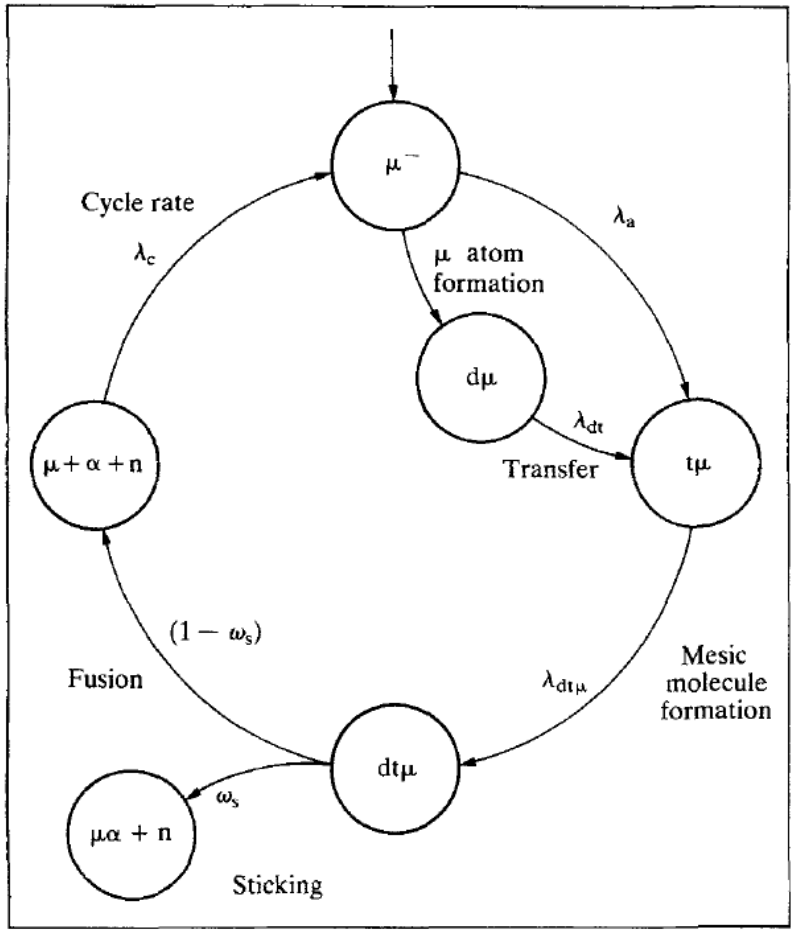
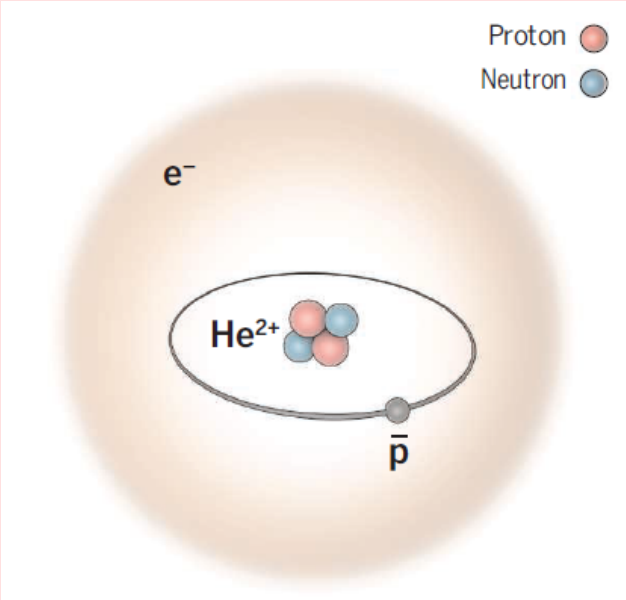


Figure 1. The principal muon catalysis fusion cycle in a deuterium and tritium mixture.

Antiprotonic Helium



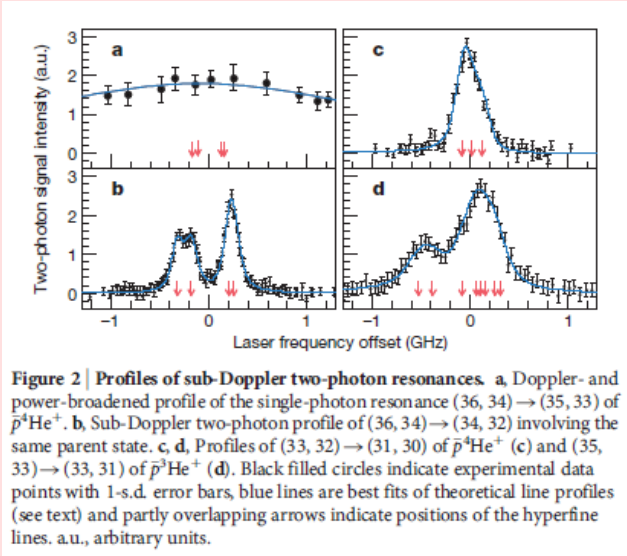


Figure 2 | Profiles of sub-Doppler two-photon resonances. **a**, Doppler- and power-broadened profile of the single-photon resonance (36, 34) → (35, 33) of $\bar{p}^4He^+$. **b**, Sub-Doppler two-photon profile of (36, 34) → (34, 32) involving the same parent state. **c**, **d**, Profiles of (33, 32) → (31, 30) of $\bar{p}^4He^+$ (**c**) and (35, 33) → (33, 31) of $\bar{p}^3He^+$ (**d**). Black filled circles indicate experimental data points with 1-s.d. error bars, blue lines are best fits of theoretical line profiles (see text) and partly overlapping arrows indicate positions of the hyperfine lines. a.u., arbitrary units.

[M. Hori et al. *Nature* **475**, *484 (2011)]*

Isotope	Transition $(n, l) \rightarrow (n-2, l-2)$	Transition frequency (MHz)	
		Experiment	Theory
$\bar{p}^4He^+$	(36, 34) → (34, 32)	1,522,107,062(4)(3)(2)	1,522,107,058.9(2.1)(0.3)
	(33, 32) → (31, 30)	2,145,054,858(5)(5)(2)	2,145,054,857.9(1.6)(0.3)
$\bar{p}^3He^+$	(35, 33) → (33, 31)	1,553,643,100(7)(7)(3)	1,553,643,100.7(2.2)(0.2)

Experimental values show respective total, statistical and systematic 1-s.d. errors in parentheses; theoretical values (ref. 3 and V. I. Korobov, personal communication) show respective uncertainties from uncalculated QED terms and numerical errors in parentheses.

$$m_{\bar{p}}/m_e = 1836.152\,6734(15) \quad [8\times10^{-10}]$$

Antiprotonic Helium in Russian Media

Lenta.ru: Главное: | Lenta.ru: Прогресс: Физик | как сделать снимок экран | Как сделать снимок экра

lenta.ru/news/2011/07/28/antiproton/

Lenta.ru | my homepage | GISMETEO.RU | Google | Википедия | РФФИ Грант-экспр... | Яндекс | Другие закладки

Главное
В России
Политика
б.СССР
В мире
Америка
Германия
Экономика
Финансы
Бизнес
О рекламе
Недвижимость
Авто
Мотор
Преступность
Масс-медиа
О высоком
Кино
Музыка
Re:Аквариум
Спорт
Прогресс
Интернет
Технологии
Игры
Оружие
Медицина
Из жизни

28.07.2011, 14:46:17

Версия для печати | PDA/КПК



Антипротонный деселератор, который ученые использовали для работы. Фото CERN

Физики взвесили антипротоны в атомкулах

Группа ученых Масаки Хори (Masaki Hori) из Института квантовой оптики общества Макса Планка провела наиболее точное измерение массы антипротона, улучшив известное значение на несколько порядков. Исследователи в очередной раз подтвердили, что массы протона и антипротона совпадают. Статья ученых появилась в журнале *Nature*, а ее краткое изложение приводит physicsworld.com.

В рамках исследования физики изучали так называемые атомкулы - экзотические молекулы гелия, в которых один из электронов замещен антипротоном. Эти объекты, способные существовать несколько микросекунд и получившие название антипротонного гелия, были открыты в 1991 году японскими физиками.

Последние новости

17.10 18:48 Удальцова отпустили под подписку о невыезде

17.10 18:26 Организаторы выборов в КС заявили о сохранности денег участников МММ

17.10 18:46 Власти Москвы проследят за митингами оппозиции

17.10 19:46 Госдума одобрила законопроект об образовании

17.10 19:13 Пивоваров обвинил Мамонтова в искажении смысла "Срока"

17.10 20:19 Посольство США в Стокгольме возобновило работу после эвакуации

17.10 19:59 В Сирии подбитый вертолет взорвался в воздухе

Аутсайд

Розовый жираф: Нобелевский успех закоренелого двоечника и его мамы
Нынешний нобелевский лауреат сэр Джон Гёрдон, оказывается, был закоренелым двоечником.

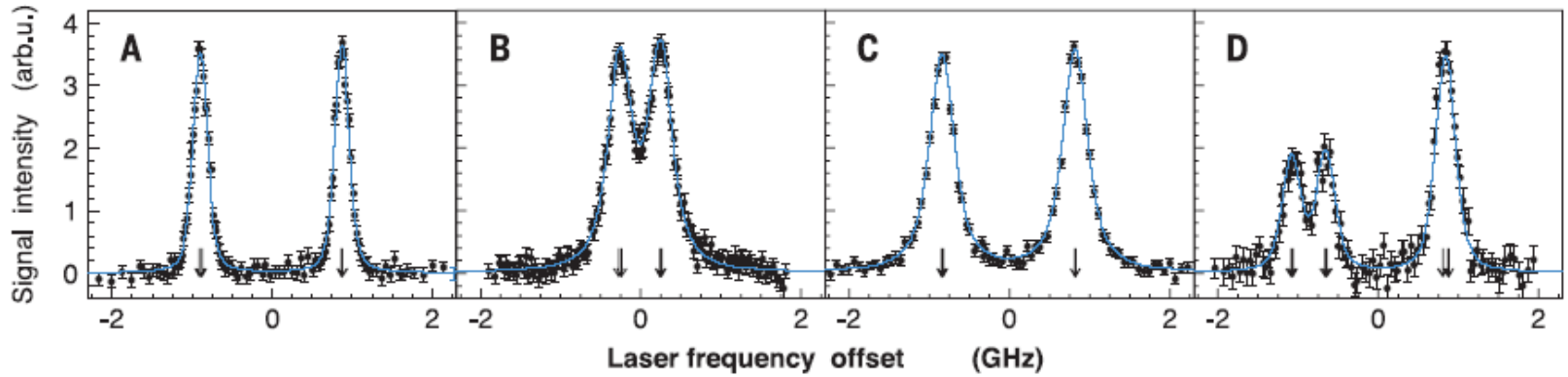
Science: Dance Your Ph.D. Finalists Announced
Финалисты конкурса "Станцуй свою диссертацию", объявленного престижным научным журналом, пытаются... станцевать свою диссертацию.

BBC News: Bloodhound land speed rocket test roars over Newquay
Захватывающее видео подготовки к тесту аппарата Bloodhound, похожего скорее на ракету, чем на суперкар.

New Scientist: Reality revealed: The ultimate fabric of the universe
NewScientist пытается за две с половиной минуты рассказать, из чего состоит реальность и приходит к весьма неожиданному выводу

Modern status. Experiment

Masaki Hori *et al.* Science **354**, 610 (2016)



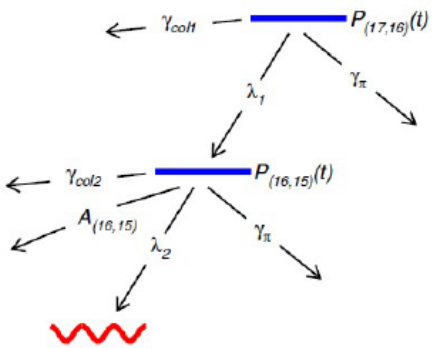
$$m_{\bar{p}}/m_e = 1836.152\,6734(15) \quad [8\times10^{-10}]$$

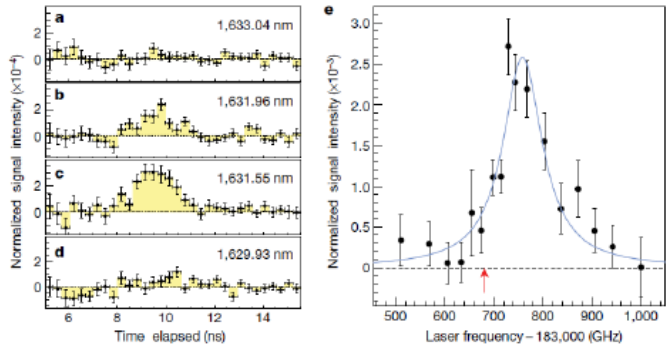
Precision Spectroscopy of the Pionic Helium-4

Zhi-Da Bai, V.I. Korobov et al., Phys. Rev. Lett. **128**, 183001 (2022)

The theoretical transition frequency of $(n, l) = (17, 16) \to (16, 15)$ in pionic helium-4 may be calculated to an accuracy of 4 ppb, that includes relativistic and quantum electrodynamic corrections up to $O(R_\infty \alpha^5)$. Once measurements reach the ppb level, then the accuracy of determining the **pionic mass** can achieve a relative precision of 10^{-8}.

Outcome: **Such a high precision value of m_π can impose direct experimental constraints on the mass of the antineutrino of muon flavor.**





Laser resonance signals of the transition
(n, l) = (17, 16) → (17, 15) in metastable π^4He^+ atoms.
M.Hori et al. Nature 581, 37 (2020)

Thank you for your attention!